Accurate First-Principles Detailed-Balance Determination of Auger Recombination and Impact Ionization Rates in Semiconductors

S. Picozzi
Istituto Nazionale di Fisica della Materia (INFM), Dipartimento Fisica, Università L'Aquila, 67010 Coppito (L'Aquila), Italy

R. Asahi
Toyota Central R & D Labs., Inc., Nagakute, Japan

C. B. Geller
Bettis Atomic Power Laboratory, West Mifflin, Pennsylvania 15122

A. J. Freeman
Department Physics and Astronomy and Materials Research Center, Northwestern University, Evanston, Illinois 60208
(Received 8 January 2002; published 21 October 2002)

The technologically important prediction of Auger recombination lifetimes in semiconductors is addressed by means of a fully first-principles formalism, based on precise energy bands and wave functions provided by the full-potential linearized augmented plane wave code. The minority carrier Auger lifetime is determined by two related approaches: (i) a direct evaluation within Fermi's golden rule, and (ii) an indirect evaluation, based on a detailed balance formulation combining Auger recombination and its inverse process, impact ionization, in a unified framework. Lifetimes determined with the direct and indirect methods show excellent consistency between them (i) for n-doped GaAs and (ii) with measured values for GaAs and InGaAs. This indicates the computational formalism as a new sensitive tool for use in materials performance optimization.

DOI: 10.1103/PhysRevLett.89.197601 PACS numbers: 79.20.Fv, 71.15.Mb, 79.20.Ap

Led by advances in computational simulation, the paradigm within semiconductor device engineering is shifting away from the static perspective of material properties as design "constraints" towards a more empowering view of material properties as design optimization parameters [1,2]. However, despite the fundamental importance of these processes, owing to a lack of adequate capability for their prediction, carrier recombination processes have remained largely beyond the reach of materials design. Minority carrier lifetime is a critical, performance-limiting material parameter in many optoelectronic devices. Two recombination processes—radiative and Auger—generally impose theoretical and practical limits on lifetimes. Minority carrier lifetimes in heavily doped and/or narrow band gap materials (such as 1.6 μm $In_{0.53}Ga_{0.47}As$, a basic material for thermophotovoltaic devices) tend to be limited by Auger recombination (AR), and so its first-principles determination is the focus of this paper.

In n-doped, direct band gap materials, the dominant Auger process is electron-electron-hole (e^--e^--h) recombination [3]. As shown in Fig. 1(a), in the e^--e^--h process, a valence band hole decays via nonradiative recombination with a conduction electron, conserving energy and momentum through transfer to a second conduction e^-. In the inverse process of e^- initiated impact ionization (I-I) [Fig. 1(b)], an energetic primary e^- promotes a secondary valence e^- into the conduction band, producing a mobile e^--h pair.

In this work, the fully first-principles approach that was used successfully to evaluate I-I rates [4] is extended to the calculation of AR rates which are found to be in good agreement with experimental and theoretical values reported for the most studied direct semiconductor, GaAs, and for technologically important InGaAs. Moreover, AR lifetimes calculated via Fermi's golden rule are shown to be strikingly consistent with those determined via detailed balance principles proceeding from calculated I-I rates. To our knowledge, this density functional theory (DFT) [5] study represents the first fully *ab initio* determination of AR lifetimes. The agreement of

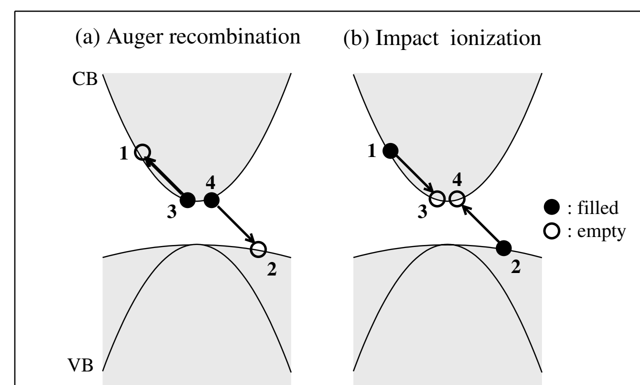

FIG. 1. Simulated processes in n-type materials: (a) AR, resulting in a hole decay; (b) electron-initiated I-I, resulting in a pair production.

 © 2002 The American Physical Society

computational results with experiment for n-type GaAs and $In_{0.5}Ga_{0.5}As$ indicates that this method is sufficiently precise and reliable to correctly predict trends of the Auger coefficient as a function of physical parameters. Since the current approach is all-electron and *ab initio* in nature, we expect the same method to be equally successful for new and more complex materials. Finally, we find that detailed balance evaluations appear to be a computationally efficient means of determining AR rates.

Within an independent particle scheme [6], given a hole in state $(n_2, \mathbf{k_2})$, the AR rate is expressed as

$$R^{AR}(n_2, \mathbf{k_2}) = 2\frac{2\pi}{\hbar}\sum_{n_3,n_4}\int d^3\mathbf{k_3}\int d^3\mathbf{k_4}|M|^2 f(E^{n_4}_{\mathbf{k_4}})f(E^{n_3}_{\mathbf{k_3}})g(E^{n_1}_{\mathbf{k_1}})\delta(E^{n_3}_{\mathbf{k_3}} + E^{n_4}_{\mathbf{k_4}} - E^{n_1}_{\mathbf{k_1}} - E^{n_2}_{\mathbf{k_4}}) \quad (1)$$

and the total AR rate is

$$R^{\mathrm{AR}} = \sum_{n_2}\int d^3\mathbf{k_2}\, g(E^{n_2}_{\mathbf{k_2}})\, R^{\mathrm{AR}}(n_2, \mathbf{k_2}). \quad (2)$$

Here, the n_i are the band indices [n_i, $i = 1, \ldots, 7$ ($i = 5, \ldots, 11$) for GaAs (InGaAs), corresponding to the four valence and three conduction bands considered] and $\mathbf{k}_{1,3,4}$ are $\mathbf{k}$ points in the full Brillouin zone (BZ) [7]. The manyfold integration over the BZ is performed according to the Sano-Yoshii scheme [8], using 152 [9] and 126 $\mathbf{k}$ points in the irreducible wedge of the zinc blende and tetragonal BZ, respectively [10]. The summation over $\mathbf{k}_2$ is carried out in the BZ irreducible wedge. f denotes the Fermi-Dirac occupation probability and $g = 1 - f$. The matrix elements, taking into account both *direct* and *exchange* terms (obtained from the direct contribution through the exchange of final states), are of the form $|M|^2 = \frac{1}{2}(|M_D|^2 + |M_E|^2 + |M_D - M_E|^2)$. The direct term is given as

$$M_D = \frac{4\pi e^2}{\Omega}\sum_{\mathbf{G_0},\mathbf{G_U}}\delta(\mathbf{k_3}+\mathbf{k_4}-\mathbf{k_1}-\mathbf{k_2}+\mathbf{G_0})\frac{\rho_{n_3,\mathbf{k_3};n_1,\mathbf{k_1}}(\mathbf{G_U})\rho_{n_4,\mathbf{k_4};n_2,\mathbf{k_2}}(\mathbf{G_0}-\mathbf{G_U})}{\varepsilon(q)(|\mathbf{k_1}-\mathbf{k_3}+\mathbf{G_U}|^2 + \lambda^2)}, \quad (3)$$

where e is the electronic charge and Ω is the volume of the unit cell. Energy (momentum) conservation is enforced through the δ function in the energy eigenvalues ($\mathbf{k}$ vectors) and $\rho_{n_f,\mathbf{k_f};n_i,\mathbf{k_i}}(\mathbf{G})$ is the Fourier transform of the overlap matrix of the wave functions, i.e., $\rho_{n_f,\mathbf{k_f};n_i,\mathbf{k_i}}(\mathbf{r}) = \Psi^*_{n_f,\mathbf{k_f}}(\mathbf{r})\Psi_{n_i,\mathbf{k_i}}(\mathbf{r})$. The subscripts i (f) denote initial (final) states; $q = |\mathbf{k_1}-\mathbf{k_3}+\mathbf{G_U}|$ is the momentum transfer, and $\mathbf{G_0}$ and $\mathbf{G_U}$ are reciprocal lattice vectors. The interaction between the valence and conduction electrons was described using a Coulomb interaction screened through a static model dielectric function $\varepsilon(q)$ [11]. The interaction between conduction carriers is modeled through a Debye potential, in which the inverse of the screening length is expressed as $\lambda = \sqrt{\frac{4\pi n^0 e^2}{K_B T}}$, n^0, T, and K_B being the carrier density, the temperature (here, $T = 300$ K), and the Boltzmann constant, respectively.

The theoretical estimate of the I-I rate [12] is known to be sensitive to the assumed band structure. Therefore, to faithfully reproduce experimental band structures, we employ the screened-exchange local density approximation (sX-LDA) [13,14], as implemented [15] self-consistently in the highly precise all-electron, full-potential linearized augmented plane wave (FLAPW) [16] method.

The effect of spin-orbit coupling, neglected here, was investigated in Ref. [12] for GaAs; the overall effect was shown to be relatively small. Umklapp processes for $\mathbf{G}_U = 0$ were fully included; the $\mathbf{G}_0 \neq 0$ terms, which are important at high energies, were not included, since AR is a threshold process. Phonon-assisted transitions [17,18] and many-body [19,20] effects were also not included; for InGaAs, it was shown [18] that phonon-assisted AR should not be relevant compared to the direct AR. Within these approximations, giving an estimated overall error of 30%–40% on the AR rates, we show below that our simple band-to-band AR within DFT correctly describes the physical trends as a function of technological parameters, and so may be used as a sensitive tool in materials device optimization.

It can be shown [21] that the Auger lifetime τ_p can be expressed as

$$\frac{1}{\tau_p} = \frac{R^{\mathrm{AR}}}{N_p^0}, \quad (4)$$

where N_p^0 is the number of minority carriers per unit cell at equilibrium. In Fig. 2 we show the dependence of the calculated τ_p on carrier density, approximately linear on a log-log scale and similar to previously reported trends for Si [6] and n-doped InGaAs [22].

The Auger coefficient C_n is defined by the relation

$$\frac{1}{\tau_p} = C_n(n^0)^2. \quad (5)$$

Partial recombination lifetimes usually are "determined" experimentally based on curve fits to lifetime measurements resulting from several competing recombination processes. The parabolic relationship above is the usual basis for determinations of C_n. However [6], both shifts in the Fermi energy and changes in λ introduce a carrier density dependence into Eqs. (1) and (2), so that C_n itself is expected to depend on n^0. This is actually the case from our calculations. Indeed, in GaAs our C_n, determined as the ratio of the inverse lifetime and n^0 squared, ranges from $2.3 \times 10^{-30}\ \mathrm{cm}^6\,\mathrm{s}^{-1}$ at $n^0 \sim 4 \times 10^{15}\ \mathrm{cm}^{-3}$ to $0.5 \times 10^{-30}\ \mathrm{cm}^6\,\mathrm{s}^{-1}$ at $n^0 \sim 6 \times 10^{16}\ \mathrm{cm}^{-3}$.

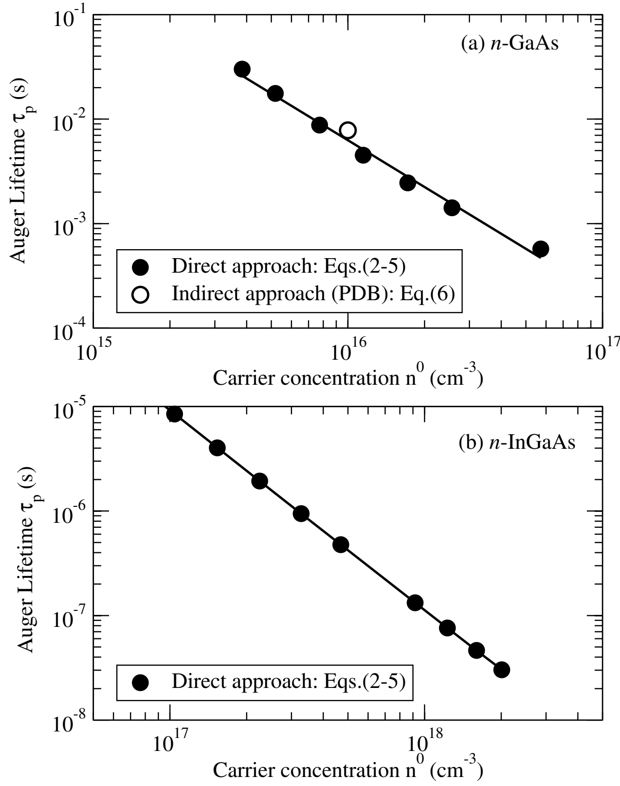

FIG. 2. Calculated hole Auger lifetime vs carrier concentration in (a) GaAs and (b) InGaAs. The results for the binary compound are obtained according to the direct approach [see Eqs. (2)–(5)–filled circles] and to the indirect approach [see Eq. (6)—open circle].

This range of values is compared in Table I with previous experimental [23–25] and theoretical [26,27] results. In InGaAs, there is only a slight dependence of C_n on n^0, C_n ranging from 0.8×10^{-29} cm^6 s^{-1} to 1.1×10^{-29} cm^6 s^{-1} for concentrations ranging from 7×10^{16} cm^{-3} to 2×10^{18} cm^{-3}. These values are compared in Table II with previous experimental [22,28,29] and theoretical [30,31] results. The comparison between the calculated values for GaAs and InGaAs shows that there is a strong reduction of C_n, suggesting that AR is crucial in the narrow-gap InGaAs. Despite the wide range over which the reported C_n vary, the calculated trend with Ga content is confirmed experimentally, unambiguously emphasizing the power of DFT in predicting both quantitatively and qualitatively correct physical trends as a function of doping, composition, etc. Our result for C_n is in good agreement with most of the experimental values and with previous model calculations incorporating various simplifications [26,27]. All considered, we conclude that our results confirm the reliability of the computational methods herein described (i) to accurately calculate AR lifetimes that cannot be easily determined by experiment; (ii) for mapping trends with respect to material composition and dopant density, that are useful to guide device and materials design; and (iii) for describing AR in novel and more complex materials.

AR and I-I are related as inverse microscopic processes through the principle of detailed balance (PDB), in the same manner as optical emission and absorption. In fact, in the radiative (nonradiative) case, the *e-h* generation process is the absorption (I-I), in which the initial object is the photon (highly energetic impacting electron); correspondingly, their inverse recombination process is emission (AR), in which the final product is the photon (Auger electron).

Following Landsberg [3], the AR lifetime, τ_p, is given by

$$\frac{1}{\tau_p} \sim \frac{1}{N_p^0} \sum_{n_1} \int d^3\mathbf{k_1} \beta(n_1, \mathbf{k_1}) R^{\text{I-I}}(n_1, \mathbf{k_1}) f(n_1, \mathbf{k_1}), \quad (6)$$

where $\beta(n_1, \mathbf{k_1})$ is a factor (≤ 1) that takes into account the occurrence of processes from state $(n_1, \mathbf{k_1})$ other than I-I and the $R^{\text{I-I}}(n_1, \mathbf{k_1})$ are the I-I rates. This last expression is the nonradiative equivalent of the van Roosbroeck-Shockley relation [32], that has been used extensively in determinations of radiative recombination lifetimes from the complex dielectric function. However, while experimental dielectric function data are abundant and reliable, experimental data for *e*-initiated I-I rates are normally inadequate to estimate τ_p from Eq. (6). A utility of the current formalism is that one can calculate both I-I and AR rates either independently from first-principles, or from one another via PDB arguments. In

TABLE I. Auger coefficients in *n*-type GaAs.

Experimental technical or theoretical approach	C_n (cm^{6}s^{-1})
sX-LDA FLAPW	$(0.5 \leq C_n \leq 2.3) \cdot 10^{-30}$
Photoacoustic[a]	$1.3 \cdot 10^{-30}$
Time-resolved photoluminescence (TRPL) decay[b]	$(7 \pm 4) \cdot 10^{-30}$
TRPL decay[c]	Upper limit of $1.6 \cdot 10^{-29}$
Nonparab. bands + phonon assisted + eff. masses[d]	$4.7 \cdot 10^{-30}$
Nonparab. bands + phonon assisted + $\mathbf{k \cdot p}$[e]	$1.5 \cdot 10^{-31}$

[a]Reference [25]. [b]Reference [24]. [c]Reference [23]. [d]Reference [27]. [e]Reference [26].

TABLE II. Auger Coefficients in n-type InGaAs.

Experimental technical or theoretical approach	C_n ($cm^6 s^{-1}$)
sX-LDA FLAPW	$(0.8 \leq C_n \leq 1.1) \cdot 10^{-29}$
TRPL decay[a]	$0.5 \cdot 10^{-29}$
Radio-frequency photoconductive decay[b]	$7 \cdot 10^{-29}$
PL photon counting[c] +degenerate conditions	$18 \cdot 10^{-29}$
Nonparab. bands+ phonon assisted+eff. masses[d]	$0.5 \cdot 10^{-29}$
Kane model for wave functions[e]	$3 \cdot 10^{-29}$

[a]Reference [28]. [b]Reference [29]. [c]Reference [22]. [d]Reference [30]. [e]Reference [31].

our formalism, we focus on two selected processes (I-I and AR), each being the inverse of the other; therefore, the PDB holds with $\beta(n_1, \mathbf{k_1}) = 1$ [or, equivalently, that every energetic electron in state $(n_1, \mathbf{k_1})$ initiates I-I]. In Fig. 2, Eq. (6) is applied to the previously calculated I-I rates [4] and the Auger lifetime for $n^0 = 1.0 \times 10^{16}$ cm^{-3} is derived. The open symbol in Fig. 2 denotes the value obtained, which is in striking agreement with the values calculated using the direct approach [see Eq. (1)]. The excellent agreement achieved between the direct and "indirect" calculations provides confidence in the equivalency of the two approaches and in the numerical procedures embodied therein.

In summary, we have presented a fully first-principles formalism for calculating Auger recombination lifetimes using self-consistent screened-exchange FLAPW quasiparticle wave functions and band structures. The numerical accuracy of the approach was checked using the PDB applied to the two simulated processes, I-I and AR. The Auger lifetime was determined using two equivalent approaches, "direct" and "indirect," with highly consistent results. Our results for GaAs and InGaAs are in excellent agreement with the most accurate experimental and theoretical data, providing confidence in the computational method and justifying its future applications to more complex systems.

This work at Northwestern University was supported by the National Science Foundation (through its MRSEC program at the Materials Research Center).

[1] C. B. Geller, W. Wolf, S. Picozzi, A. Continenza, R. Asahi, W. Mannstadt, A. J. Freeman, and E. Wimmer, Appl. Phys. Lett. **79**, 368 (2001).
[2] A. Franceschetti and A. Zunger, Nature (London) **402**, 60 (1999).
[3] P.T. Landsberg, *Recombination in Semiconductors* (Cambridge University Press, Cambridge, 1991).
[4] See S. Picozzi, R. Asahi, C. B. Geller, A. Continenza, and A. J. Freeman, Phys. Rev. B, **65**, 113206 (2002), where we report further computational details, not repeated here.
[5] W. Kohn and L. J. Sham, Phys. Rev. **140**, A1113 (1965); P. Hohenberg and W. Kohn, Phys. Rev. **136**, B864 (1964).
[6] D. B.Laks, G. F.Neumark, A. Hangleiter, and S. T. Pantelides, Phys. Rev. Lett. **61**, 1229 (1988).
[7] The calculations were performed on a single 512 Mb RAM Dec Alpha workstation in ~300 CPU hours.
[8] N. Sano and A. Yoshii, Phys. Rev. B **45**, 4171 (1992).
[9] The accuracy was tested by further increasing the k mesh: in GaAs, a (12,12,12) k grid produced rates differing at most by 8% from those obtained with the present (10,10,10) k grid.
[10] $In_{0.5}Ga_{0.5}As$ was simulated using a [001]-ordered 1×1 InAs/GaAs superlattice, with four atoms in the unit cell.
[11] G. Cappellini, R. Del Sole, L. Reining, and F. Bechstedt, Phys. Rev. B **47**, 9892 (1993).
[12] D. Harrison, R. A. Abram, and S. Brand, J. Appl. Phys. **85**, 8178 (1999); **85**, 8186 (1999).
[13] B. M. Bylander and L. Kleinman, Phys. Rev. B **41**, 7868 (1990).
[14] A. Seidl, A. Gorling, P. Vogl, J. A. Majewski, and M. Levy, Phys. Rev. B **53**, 3764 (1996).
[15] R. Asahi, W. Mannstadt, and A. J. Freeman, Phys. Rev. B **59**, 7486 (1999); **62**, 2552 (2000).
[16] E. Wimmer, H. Krakauer, M. Weinert, and A. J. Freeman, Phys. Rev. B **24**, 864 (1981).
[17] M. Takeshima, Phys. Rev. B **23**, 6625 (1981).
[18] R. J. Dutta and N. K. Nelson, J. Appl. Phys. **85**, 74 (1982).
[19] M. Takeshima, Phys. Rev. B **28**, 2039 (1983); **29**, 1993 (1984).
[20] J. Bude, K. Hess, and G. J. Iafrate, Phys. Rev. B **45**, 10 958 (1992).
[21] S. Krishnamurthy, A. Sher, and A. B. Chen, J. Appl. Phys. **82**, 5540 (1997).
[22] W. K. Metzger *et al.*, Appl. Phys. Lett. **79**, 3272 (2001).
[23] E. Marin *et al.*, J. Appl. Phys. **83**, 2604 (1998).
[24] U. Strauss, W.W. Rühle, and K. Köhler, Appl. Phys. Lett. **62**, 55 (1993).
[25] G. B. Lush *et al.*, J. Appl. Phys. **72**, 1436 (1992).
[26] A. Haug, J. Phys. C **16**, 4159 (1980).
[27] M. Takeshima, Jpn. J. Appl. Phys. **22**, 491 (1983).
[28] C. H. Henry, R. A. Logan, F. R. Merritt, and C. G. Betha, Electron. Lett. **20**, 358 (1984).
[29] R. K. Ahrenkiel, R. Ellingson, S. Johnston, and M. Wanlass, Appl. Phys. Lett. **72**, 3470 (1998).
[30] M. Takeshima, J. Appl. Phys. **56**, 691 (1984).
[31] W. Bardyszewski and D. Yevick, J. Appl. Phys. **58**, 2713 (1985).
[32] W. Van Roosbroeck and W. Shockley, Phys. Rev. **94**, 1558 (1954).